J. Phys. B: Atom. Molec. Phys. 13 (1980) 2309–2325. Printed in Great Britain

The $1^1S \rightarrow 2^1S$ and $1^1S \rightarrow 2^1P$ excitation of helium by electron impact

W C Fon†, K A Berrington and A E Kingston

Department of Applied Mathematics and Theoretical Physics, The Queen's University of Belfast, Belfast, BT7 1NN, Northern Ireland

Received 26 November 1979

Abstract. The *R*-matrix method calculations of Berrington *et al* and Fon *et al* are extended to the energy ranges $21{\cdot}4 < E < 30$ eV and $80 < E \leqslant 200$ eV for the electron impact excitation of 2^1S and 2^1P states of helium. Differential and integrated cross sections for these transitions and the (λ, χ) parameters for the 2^1P excitation are calculated and compared with the recent theoretical calculations and experimental measurements.

1. Introduction

In the past, theories of electron impact excitation were mainly applied to calculating integrated cross sections. However, it is very misleading to judge the success of a theoretical model purely on the agreement of the integrated cross sections with experimental measurements. For the $1^1S \rightarrow 2^1S$ and $1^1S \rightarrow 2^1P$ excitations of helium by electron impact in the intermediate energy range, the angular distribution of the scattered electron for these excitation processes decreases very steeply as the scattering angle of the electron increases and hence the main contribution to the integrated cross sections comes from the smaller scattering angles. Hence it is not surprising that a simple method like the first Born approximation might give reasonable agreement with experiments for integrated cross sections, and yet diverge from the measurements of angular distribution by orders of magnitude at large scattering angles. Recently a number of measurements of differential cross sections have become available and we are in a better position to understand in detail the mechanism which is responsible for the scattering process.

Useful experimental measurements are now available on angular correlations. Angular correlations between the scattered electrons resulting from the excitation of the 2^1P state of helium and the photons emitted in the de-excitation of the state were first studied by Eminyan *et al* (1974) using a coincident technique for an incident electron energy of 80 eV. From the measured angular correlations, the orientation and alignment parameters can be extracted without the need for normalisation. There are now a number of measurements (e.g. Tan *et al* 1977, Ugbabe *et al* 1977, Hollywood *et al* 1979, Sutcliffe *et al* 1978). There is agreement between various experimental groups for small electron scattering angles: however, the measurements of Sutcliffe *et al* (1978)

† On leave of absence from: The Department of Mathematics, University of Malaya, Pantai Valley, Kuala Lumpur, Malaysia.

(repeated by Steph and Golden 1980) and those of Hollywood *et al* (1979) are in disagreement at large electron scattering angles.

In the intermediate energy range the excitation of the $n=2$ states of helium has been reviewed by Bransden and McDowell (1978). Most of the calculations are based on the distorted-wave approximation (e.g. Madison and Shelton 1973, Scott and McDowell 1976, Thomas *et al* 1974, Baluja and McDowell 1979). At high energies, the eikonal-Born series method (Byron and Joachain 1975), the Glauber approximation (Terebey 1974, Yates and Tenney 1972), the two-potential method (Gupta and Mathur 1979), the second-order-potential method (Bransden and Winters 1975, Winters *et al* 1977) and the ten-channel eikonal approximation (Flannery and McCann 1975) are also being applied with considerable success. Reasonable success has been achieved with the calculations of Thomas *et al* (1974) and Madison and Shelton (1973) in predicting the differential cross sections for 2^1P excitation; however, they are less successful in reproducing the experimental shape of the differential cross sections for 2^3S and 2^3P excitation. The distorted-wave calculation of Madison and Shelton (1973) is known to be sensitive to the target wavefunction chosen (Bransden and McDowell 1978). While the DW calculation of Baluja and McDowell (1979) has successfully improved on the calculation of Scott and McDowell (1976), they fail to predict correctly the shape of the differential cross section for 2^3S excitation. No theoretical methods have produced all round satisfactory predictions for all excitations of $n=2$ states of helium in the experimental shape of the cross sections versus energy and differential cross sections versus angle (Bhadra *et al* 1979). There is also serious disagreement among theoretical calculations in predicting (λ, χ) parameters for 2^1P excitation, particularly over large angles where no theoretical results give agreement with experimental measurements.

Recently Berrington *et al* (1975) and Fon *et al* (1978) have calculated respectively the integrated and differential cross sections for the $n=2$ states of helium by using five states in the R-matrix method. Agreement between the R-matrix method results and measurements is excellent; however, these calculations have only been carried out over a small range of energy (between $n=2$ and $n=3$ excitation thresholds). Fon *et al* (1979a) have extended these calculations to consider the 2^3S and 2^3P (spin-forbidden) excitation for energies in the $21{\cdot}4 \leqslant E \leqslant 30$ eV and $80 < E \leqslant 200$ eV ranges. The agreement between this calculation and experiments is encouraging. In this paper, we present the five-state R-matrix results for the 2^1S and 2^1P excitations over the same energy ranges as considered by Fon *et al* (1979a).

2. *R*-matrix calculations

In this paper, we extend the earlier calculations of Berrington *et al* (1975) and Fon *et al* (1978, 1979a,b) to energies up to 200 eV for electron excitation of the 2^1S and 2^1P states from the ground state of helium. We adopt the same R-matrix radius $a = 16{\cdot}044$ au and the number of continuum orbitals included for each angular momentum is 25. The calculations were carried out retaining the first five atomic eigenstates (1^1S, 2^3S, 2^1S, 2^3P, 2^1P) which were represented by the same CI wavefunctions as in the earlier works. In contrast to the spin-forbidden 2^3S and 2^3P excitations, in which only low partial waves contribute to the calculation of cross sections, a large number of partial waves are required to give convergence for the 2^1P differential cross sections and (λ, χ) parameters for 2^1P excitation. This is due to the long-range dipole character of the interaction resulting from the coupling between the S state and the P state. Typically, at 200 eV (the highest energy considered in this paper), 95 partial waves are included; only the first 14 partial waves are calculated from the R-matrix program, the next ten partial waves were extrapolated to give smooth convergence to the T-matrix elements obtained by a five-state unitarised Born approximation. T-matrix elements for the remaining higher partial waves are obtained by a five-state unitarised Born approximation using the same CI wavefunctions as in the R-matrix program.

One difficulty in our calculations arises from the inclusion of correlation terms in the expansion of our total wavefunction (see Fon *et al* 1979a). These terms are included for completeness and in addition they allow for short-range correlation effects at low energies when all three electrons are close together near the nucleus. If these terms were to be excluded, the R-matrix method would then be equivalent to the close-coupling approximation. Bhadra *et al* (1979) have carried out a similar five-state close-coupling approximation in the energy range $30 \leqslant E \leqslant 100$ eV. It covers the energy range where the correlation terms in R-matrix calculations give rise to spurious resonances which make the extraction of accurate results difficult.

3. Results and discussion

We have calculated the total and differential cross sections for the singlet transitions

$$e + He(1^1S) \rightarrow e + He(2^1S)$$

and

$$e + He(1^1S) \rightarrow e + He(2^1P)$$

at impact energies ranging from 1·6 eV above the 2^1S threshold to 200 eV. The orientation and alignment parameters for the 2^1P excitation are also calculated.

The basic scattering data generated in this calculation, for example the reactance matrix elements, have been stored in a computerised databank at the SRC Daresbury Laboratory. These data are more comprehensive than the tables and graphs given in this paper, and interested readers should contact the authors for further information.

Integrated cross sections at various energies for the 2^1S and 2^1P excitation are given in table 1. The excitation cross sections are higher than experimental values but are considerably lower than those of the five-state close-coupling calculation of Bhadra *et al* (1979).

3.1. $1^1S \rightarrow 2^1S$ differential cross sections

Our calculated differential cross sections for the $1^1S \rightarrow 2^1S$ excitation are displayed in table 2, and they are compared with experimental measurements and with other theoretical calculations in figures 1–3.

The general features of our angular dependence for the 2^1S excitation are:

(i) a sharp, deep minimum at low energies which becomes shallower at higher energies;

(ii) a forward peak at all energies which becomes sharper with increasing energy;

(iii) the magnitude of the backward scattering amplitude falls rapidly with increasing energy.

Table 1. Integral cross sections for 2^1S and 2^1P excitation in units of πa_0^2.

	2^1S			2^1P		
E (eV)	(*a*)	(*b*)	(*c*)	(*a*)	(*b*)	(*c*)
26·5	0·0591	—	—	0·0594	—	—
29·6†	0·0551	0·0958	0·0246	0·0865	0·122	0·0426
40·1	—	0·0656	0·0222	—	0·169	0·0751
60	—	0·0460	0·0181	—	0·183	0·1082
80‡	0·0326	0·0362	0·0155	0·1605	0·176	0·1154
100	0·0236	0·0302	0·0146	0·149	0·163	0·1148
120	0·0196	—	—	0·139	—	0·1095
150	0·0160	—	0·0121	0·126	—	0·1044
200	0·0125	—	0·00955	0·109	—	0·0944

(*a*) Present five-state R-matrix calculations.
(*b*) Five-state close-coupling calculations (Bhadra *et al* 1979).
(*c*) 2^1S: experimental values estimated by de Heer and Jansen (1977). 2^1P: experimental values of Westerveld *et al* (1979).
† Experimental values are measured at 30 eV.
‡ Present five-state R-matrix calculations at 81·63 eV.

Table 2. Differential cross section for $1^1\mathrm{S}\rightarrow 2^1\mathrm{S}$ (in units of 10^{-19} cm^2 sr^{-1}). Energy of incident electron E (eV).

Angle (deg) \ E (eV)	26·5	29·6	81·63	100	120	150	200
0	3·203^{1}	3·857^{1}	1·332^{2}	1·402^{2}	1·498^{2}	1·548^{2}	3·060^{2}
10	2·654^{1}	2·955^{1}	3·606^{1}	2·933^{1}	2·598^{1}	2·372^{1}	2·165^{1}
20	1·504^{1}	1·332^{1}	8·577	8·321	8·208	7·493	5·872
30	5·557	3·267	3·392	2·859	2·426	1·827	8·845^{-1}
40	1·075	2·678^{-1}	1·511	1·154	9·971^{-1}	7·889^{-1}	5·784^{-1}
50	1·133^{-1}	1·681^{-1}	1·268	9·509^{-1}	7·865^{-1}	5·818^{-1}	3·479^{-1}
60	5·038^{-1}	4·604^{-1}	1·338	9·362^{-1}	7·142^{-1}	4·819^{-1}	2·606^{-1}
70	1·080	5·874^{-1}	1·378	8·697^{-1}	6·049^{-1}	3·680^{-1}	1·793^{-1}
80	1·563	7·047^{-1}	1·325	7·679^{-1}	5·025^{-1}	2·882^{-1}	1·373^{-1}
90	2·083	1·054	1·254	6·777^{-1}	4·210^{-1}	2·337^{-1}	1·055^{-1}
100	2·833	1·797	1·189	5·903^{-1}	3·435^{-1}	1·797^{-1}	7·530^{-2}
110	3·870	2·992	1·138	5·323^{-1}	3·024^{-1}	1·565^{-1}	6·18^{-2}
120	5·088	4·577	1·113	4·847^{-1}	2·641^{-1}	1·302^{-1}	5·18^{-2}
140	7·220	8·130	1·108	4·313^{-1}	2·232^{-1}	1·053^{-1}	3·73^{-2}
160	8·160	1·081^{1}	1·127	4·068^{-1}	1·991^{-1}	8·92^{-2}	3·16^{-2}
180	8·311	1·175^{1}	1·132	3·924^{-1}	1·92^{-1}	8·38^{-2}	2·95^{-2}

The superscript denotes the power of ten by which the number should be multiplied.

Figure 1 compares our calculated differential cross section at 2 eV above the 2^1S threshold with the measurements of Pichou *et al* (1976). There is excellent agreement between theory and experiment.

In figure 2, our calculation for 2^1S excitation at 29·6 eV is compared with experiment and other theoretical calculations. The measurements of Hall *et al* (1973) and Trajmar (1973) are consistent in that both have a minimum at 50°. The many-body

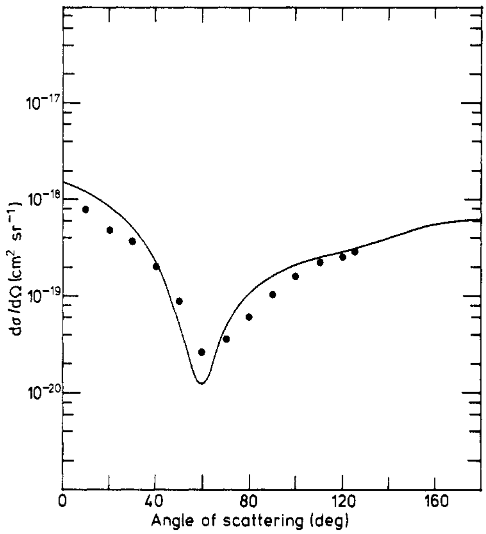

Figure 1. Differential cross section for the process: $e + He(1^1S) \rightarrow e + He(2^1S)$ at an electron energy 1·6 eV above the 2^1S threshold. Theory: ——, present R-matrix calculation. Experiment: ●, Pichou *et al* (1976).

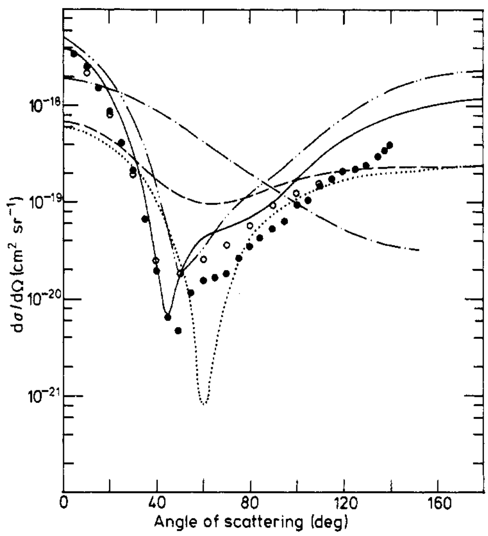

Figure 2. $1^1S \rightarrow 2^1S$ differential cross section at 29·6 eV. Theory: ——, present R-matrix five-state calculation; · · · · ·, Thomas *et al* (1974); – – –, Scott and McDowell (1975); –·–·–, first Born approximation; –··–, close-coupling five-state calculation (Bhadra *et al* 1979). Experiment: ○, Hall *et al* (1973); ●, Trajmar (1973).

theory calculation of Thomas *et al* (1974) and the DWPO calculation of Scott and McDowell (1975) show a minimum at 60°. The minimum predicted by Thomas *et al* (1974) occurs at a higher angle than the observed minimum, and the depth of the minimum is substantially lower than the measurements. The minimum predicted by Scott and McDowell is wider and shallower than the observed minimum. The cross sections for the forward scattering predicted by these two calculations are very much smaller than the experiments. Although the five-state close-coupling calculation of Bhadra *et al* (1979) exhibits the general feature of the experiments, the present R-matrix calculation appears to be in closer agreement with the experiments than any of the other theoretical predictions. Our calculated differential cross sections at 29·6 eV shown in figure 2 manifest clearly the forward peaking behaviour and show the unmistakable presence of a sharp minimum at 45°. Another interesting feature of our calculation is the formation of a shoulder at 60° which was observed by Trajmar (1973). The forward peaking behaviour and the presence of a minimum also show up in our calculations at much lower energy (see figure 1), which is in close accord with the measurements of Pichou *et al* (1976). As the incident energy increases, this minimum turns into a bend and fades away altogether at 200 eV; however, the forward peak becomes sharper and sharper as the incident energy increases.

At incident electron energies above 81 eV, a substantial discrepancy exists between our calculations and the experiments of Opal and Beaty (1972), Suzuki and Takayanagi (1973) and A Yagashita (1978, private communication) particularly at large angles of scattering. Our calculations are higher than the experimental measurements. As the impact energy increases, this discrepancy gradually disappears and there is good agreement between our calculation and the experiments at 150 and 200 eV (see figure

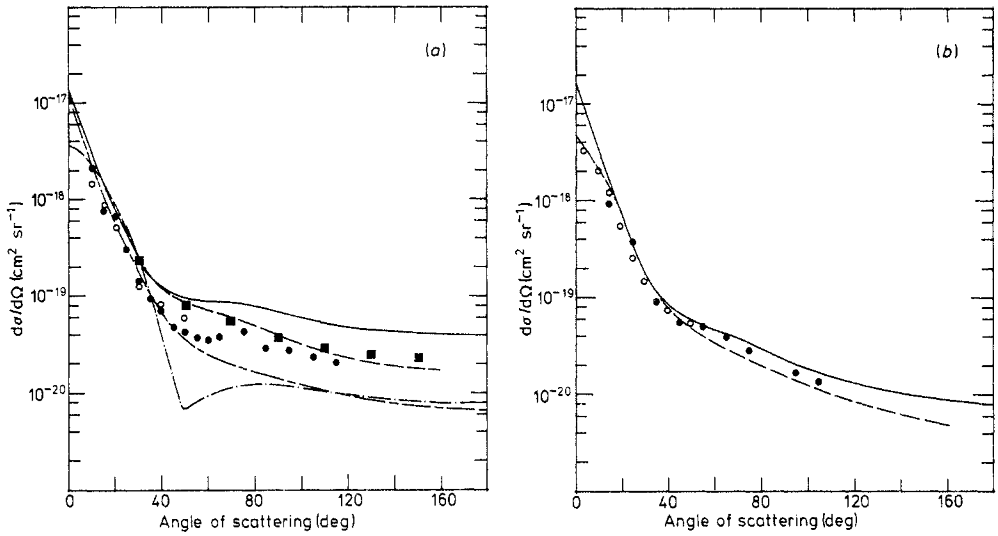

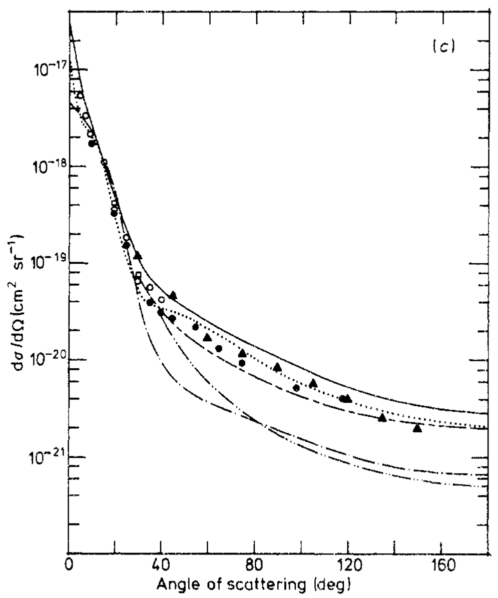

Figure 3. Same as figure 2 except that the energies are (*a*) 100 eV; (*b*) 150 eV; (*c*) 200 eV. Theory: ——, present *R*-matrix five-state calculation; –·–·–, DWPO calculation of Scott and McDowell (1975); –··–, Hidalgo and Geltman (1972); – – –, Bransden and Winters (1975); ——— , Winters *et al* (1977); ·····, Byron and Joachain (1975). Experiment: ●, Suzuki and Takayanagi (1973); ○, Yagishita (1978); ▲, Opal and Beaty (1972); □, Dillon and Lassettre (1975); ■, Crooks (1972).

3). Our calculations at 100, 150 and 200 eV are shown in figure 3, where they are compared with other theoretical calculations and measurements.

3.2. $1^1S \rightarrow 2^1P$ excitation

The $1^1S \rightarrow 2^1P$ transition is an allowed, electric dipole transition. This transition is of particular interest as it is the process about which we have the most detailed experimental data, and it is often used as a standard on which absolute calibration may be made (Chamberlain *et al* 1970). In addition to differential cross section data (Trajmar 1973, Hall *et al* 1973, Chamberlain *et al* 1970, Suzuki and Takayanagi 1973, Chutjian and Srivastava 1975, Opal and Beaty 1972), there are now several independent measurements of the angular correlation parameters λ and χ (Eminyan *et al* 1974, Ugbabe *et al* 1977, Tan *et al* 1977, Sutcliffe *et al* 1978, Hollywood *et al* 1979). We shall examine our calculation of the differential cross section and the orientation and alignment parameters separately.

3.2.1. $1^1S \rightarrow 2^1P$ differential cross section. For the $1^1S \rightarrow 2^1P$ transition, the differential cross section as a function of electron scattering angle θ is sharply peaked in the forward direction, but decreases slowly and flattens out at large angles. Our calculated differential cross sections for the $1^1S \rightarrow 2^1P$ excitation by electron impact are displayed in table 3 and they are compared with experimental measurements and other theoretical calculations in figures 4–6.

Table 3. Differential cross sections for $1^1S \rightarrow 2^1P$ (in units of 10^{-19} cm^2 sr^{-1}). Energy of incident electron E (eV).

Angle (deg) \ E (eV)	26·5	29·6	81·63	100	120	150	200
0	$3{\cdot}884^1$	$7{\cdot}089^1$	$1{\cdot}074^3$	$1{\cdot}498^3$	$1{\cdot}991^3$	$2{\cdot}704^3$	$3{\cdot}838^3$
10	$3{\cdot}513^1$	$6{\cdot}221^1$	$3{\cdot}848^2$	$3{\cdot}758^2$	$3{\cdot}424^2$	$2{\cdot}896^2$	$2{\cdot}100^2$
20	$2{\cdot}621^1$	$4{\cdot}267^1$	$7{\cdot}906^1$	$5{\cdot}737^1$	$4{\cdot}023^1$	$2{\cdot}361^1$	$1{\cdot}053^1$
30	$1{\cdot}640^1$	$2{\cdot}363^1$	$1{\cdot}454^1$	8·369	4·808	2·327	$9{\cdot}019^{-1}$
40	8·884	$1{\cdot}117^1$	3·442	1·993	1·161	$6{\cdot}319^{-1}$	$2{\cdot}858^{-1}$
50	4·527	5·208	1·686	1·024	$6{\cdot}380^{-1}$	$3{\cdot}474^{-1}$	$1{\cdot}599^{-1}$
60	2·565	3·070	1·212	$7{\cdot}068^{-1}$	$4{\cdot}312^{-1}$	$2{\cdot}311^{-1}$	$1{\cdot}050^{-1}$
70	1·866	2·389	$9{\cdot}378^{-1}$	$5{\cdot}021^{-1}$	$2{\cdot}954^{-1}$	$1{\cdot}625^{-1}$	$7{\cdot}127^{-2}$
80	1·633	2·032	$7{\cdot}464^{-1}$	$3{\cdot}706^{-1}$	$2{\cdot}165^{-1}$	$1{\cdot}137^{-1}$	$5{\cdot}084^{-2}$
90	1·525	1·781	$6{\cdot}306^{-1}$	$2{\cdot}967^{-1}$	$1{\cdot}703^{-1}$	$9{\cdot}325^{-2}$	$4{\cdot}302^{-2}$
100	1·474	1·714	$5{\cdot}412^{-1}$	$2{\cdot}395^{-1}$	$1{\cdot}428^{-1}$	$7{\cdot}334^{-2}$	$3{\cdot}553^{-2}$
110	1·473	1·855	$4{\cdot}897^{-1}$	$2{\cdot}168^{-1}$	$1{\cdot}229^{-1}$	$6{\cdot}827^{-2}$	$3{\cdot}102^{-2}$
120	1·495	2·117	$4{\cdot}589^{-1}$	$1{\cdot}950^{-1}$	$1{\cdot}097^{-1}$	$6{\cdot}001^{-2}$	$2{\cdot}761^{-2}$
140	1·443	2·525	$4{\cdot}142^{-1}$	$1{\cdot}774^{-1}$	$9{\cdot}978^{-2}$	$5{\cdot}290^{-2}$	$2{\cdot}301^{-2}$
160	1·223	2·488	$4{\cdot}055^{-1}$	$1{\cdot}677^{-1}$	$9{\cdot}416^{-2}$	$5{\cdot}095^{-2}$	$2{\cdot}149^{-2}$
180	1·089	2·371	$3{\cdot}949^{-1}$	$1{\cdot}642^{-1}$	$9{\cdot}40^{-2}$	$4{\cdot}873^{-2}$	2.097^{-2}

The superscript denotes the power of ten by which the number should be multiplied.

Figure 4 compares our calculated differential cross section at 2 eV above the 2^1P threshold with the measurements of Pichou *et al* (1976). There is good agreement between theory and experiment.

In figure 5, our calculation for the 2^1P excitation at 29·6 eV is compared with experiments and other theoretical calculations. The measurements of Hall *et al* (1973) and Trajmar (1973) are in good accord with each other. Among the theoretical calculations (Madison and Shelton 1973, Thomas *et al* 1974, Scott and McDowell 1976, Bhadra *et al* 1979), the many-body theory calculation of Thomas *et al* (1974) is in best agreement with the experiments. This is also true for an impact energy of 80 eV. While the present R-matrix calculation reproduces the experimental shape of the cross section, it overestimates the cross sections by a constant factor over all angles (see figure 5). The quantitative discrepancy persists for impact energies at 81·63 eV and gradually

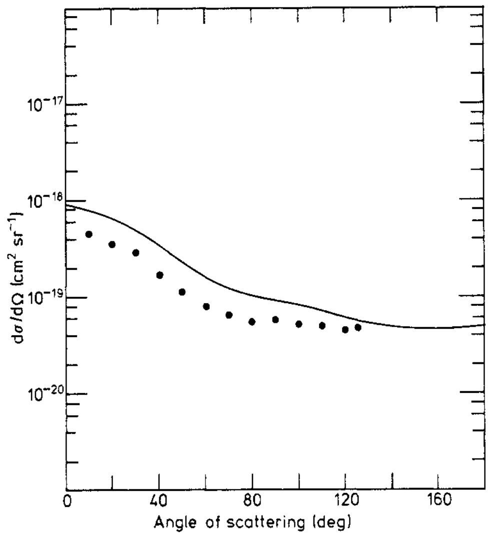

Figure 4. $1^1S \to 2^1P$ differential cross section at energy 2 eV above 2^1P threshold. Theory: ——, present R-matrix five-state calculation. Experiment: ●, Pichou *et al* (1976).

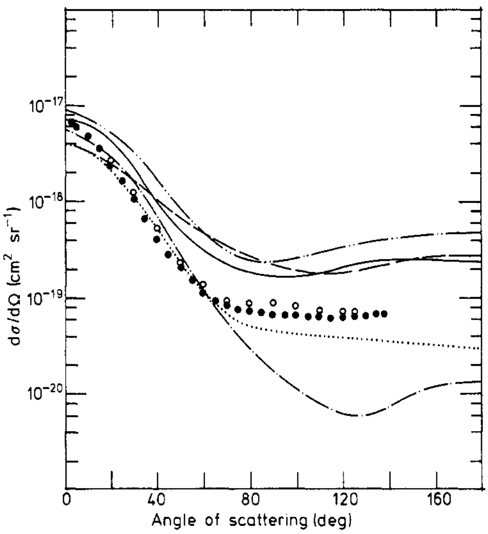

Figure 5. $1^1S \to 2^1P$ differential cross section at energy 29·6 eV. Theory: ——, present R-matrix five-state calculation; —·—·—, Scott and McDowell (1976); —··—, close-coupling five-state calculation (Bhadra *et al* 1979); – – –, Madison and Shelton (1973); · · · · ·, Thomas *et al* (1974). Experiment: ○, Hall *et al* (1973); ●, Truhlar *et al* (1973).

disappears at higher energies. There is good agreement between the present R-matrix calculations and the measurements of Suzuki and Takayanagi (1973), A Yagishita (1978, private communication) and Opal and Beaty (1972), as in the case of the 2^1S excitations, at 150 and 200 eV (see figure 6). At 200 eV, the present R-matrix calculation is in good accord with the distorted-wave calculation of Madison and Shelton (1973), the eikonal-Born series calculation of Joachain and Winters (1977); while the calculations of Winters *et al* (1977) and Scott and McDowell (1976) underestimate the cross section at large angles (see figure 6(c)).

3.2.2. $1^1S \to 2^1P$ orientation and alignment parameters. If b_m ($m = 0, \pm 1$) denotes the amplitude for scattering to the magnetic sublevels, then the differential cross sections σ_m for excitation to the magnetic sublevels are

$$\sigma_0 = |b_0|^2 \qquad \sigma_1 = \sigma_{-1} = |b_1|^2$$

and the total differential cross section $\sigma = \sigma_0 + 2\sigma_1$. In general b_m is complex and can be written as $b_m = |b_m| \exp(i\chi_m)$ where χ is the phase. The orientation and alignment parameters λ and χ are then defined as

$$\lambda = \sigma_0/\sigma \qquad 0 \leqslant \lambda \leqslant 1$$

$$\chi = \chi_1 - \chi_0 \qquad -\pi \leqslant \chi \leqslant \pi.$$

If the parameters λ and χ are known, it is not difficult to calculate the non-zero elements of the alignment tensor A^{col} and orientation vector O^{col} (Fano and Macek

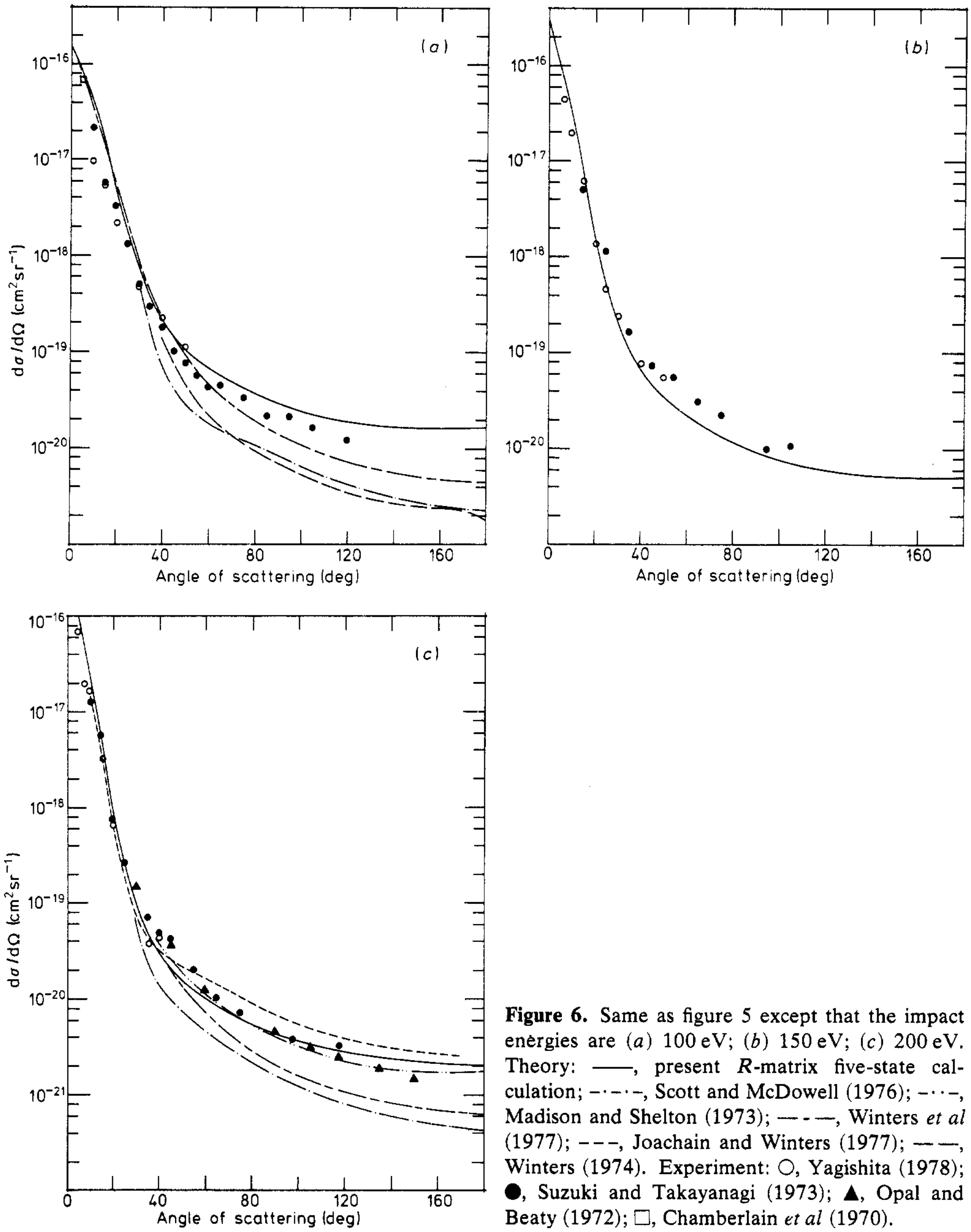

Figure 6. Same as figure 5 except that the impact energies are (*a*) 100 eV; (*b*) 150 eV; (*c*) 200 eV. Theory: ——, present *R*-matrix five-state calculation; –·–·–, Scott and McDowell (1976); –··–, Madison and Shelton (1973); — - —, Winters *et al* (1977); - - -, Joachain and Winters (1977); — —, Winters (1974). Experiment: ○, Yagishita (1978); ●, Suzuki and Takayanagi (1973); ▲, Opal and Beaty (1972); □, Chamberlain *et al* (1970).

1973); they are given by

$$A_0^{\mathrm{col}} = \tfrac{1}{2}(1-3\lambda) \tag{1}$$

$$A_{1+}^{\mathrm{col}} = [\lambda(1-\lambda)]^{1/2}\cos\chi \tag{2}$$

$$A_{2+}^{\mathrm{col}} = \tfrac{1}{2}(\lambda-1) \tag{3}$$

$$O_{1-}^{\mathrm{col}} = -[\lambda(1-\lambda)]^{1/2}\sin\chi. \tag{4}$$

In an electron–photon angular correlation measurement, if the photons are counted by a detector in the scattering plane and at 180° from the direction of the scattered electron, then the angular correlation function determined in the experiment is given by

$$N=\lambda \sin^2 \theta_\gamma+(1-\lambda)\cos^2 \theta_\gamma-2[\lambda(1-\lambda)]^{1/2} \cos\chi \sin\theta_\gamma \cos\theta_\gamma \tag{5}$$

where θ_γ is the photon scattering angle, which takes the value $\theta_{\rm min}$ when the angular correlation function is a minimum. $\theta_{\rm min}$ is given in terms of λ and χ by

$$\tan(2\theta_{\rm min})=\frac{2[\lambda(1-\lambda)]^{1/2}\cos\chi}{(2\lambda-1)}. \tag{6}$$

The calculated values of the (λ, χ) parameters are given in tables 4 and 5 at energies 26·5, 29·6, 81·63, 100, 120, 150 and 200 eV, for various values of θ_e (electron scattering angle). These parameters at 29·6 and 81·63 eV are shown in figures 7–8, where they are compared with other calculations and measurements.

There is excellent agreement among the experimental values of λ and χ at 80 eV (see figure 7) for small scattering angles (Eminyan *et al* 1974, Ugbabe *et al* 1977, Tan *et al* 1977, Sutcliffe *et al* 1978 and Hollywood *et al* 1979). However, at large scattering angles ($\theta_e > 70°$) the measurement of Sutcliffe *et al* 1978 (repeated by Steph and Golden 1980) and Hollywood *et al* (1979) are in sharp disagreement. The latter lies substantially lower than the former and exhibits a distinct minimum at 110° (see figure 7(*a*)). Over large scattering angles, it seems there is better agreement in the $|\chi|$ measurements between the experimental data of Hollywood *et al* (1979) and that of Steph and Golden (1980) in comparison to their measurements of λ. However, the large errors incurred by the measurements certainly make any comparison difficult (see figure 7(*b*)).

Table 4. Parameter λ for excitation of the 2^1P state of helium.

θ_e (deg) \ E (eV)	26·5	29·6	81·63	100	120	150	200
5	0·992	0·983	0·727	0·629	0·537	0·419	0·285
10	0·970	0·939	0·412	0·309	0·233	0·167	0·105
16	0·928	0·863	0·268	0·207	0·169	0·139	0·119
20	0·896	0·809	0·248	0·207	0·191	0·175	0·179
25	0·853	0·745	0·274	0·258	0·267	0·290	0·348
30	0·809	0·690	0·361	0·385	0·434	0·511	0·645
40	0·719	0·615	0·752	0·841	0·911	0·973	0·980
50	0·610	0·596	0·987	0·998	0·990	0·961	0·882
60	0·482	0·645	0·943	0·929	0·903	0·862	0·810
70	0·408	0·720	0·863	0·846	0·816	0·779	0·708
80	0·402	0·758	0·800	0·779	0·749	0·705	0·642
90	0·378	0·716	0·765	0·745	0·720	0·689	0·642
100	0·291	0·571	0·748	0·749	0·739	0·712	0·680
110	0·173	0·396	0·744	0·773	0·765	0·748	0·720
120	0·096	0·287	0·759	0·812	0·816	0·802	0·780
130	0·110	0·273	0·796	0·861	0·869	0·852	0·845
140	0·226	0·353	0·839	0·902	0·913	0·909	0·895
150	0·429	0·515	0·895	0·943	0·950	0·949	0·942
160	0·682	0·727	0·950	0·976	0·979	0·978	0·974
170	0·907	0·920	0·985	0·991	0·993	0·992	0·990
180	1·000	1·000	1·000	1·000	1·000	1·000	1·000

Table 5. Parameter χ (in radians) for excitation 2^1P state of helium.

θ (deg) \ E (eV)	26·5	29·6	81·63	100	120	150	200
5	−0·492	−0·501	−0·202	−0·179	−0·165	−0·163	−0·163
10	−0·489	−0·508	−0·306	−0·307	−0·308	−0·339	−0·369
16	−0·480	−0·523	−0·468	−0·488	−0·521	−0·550	−0·622
20	−0·471	−0·535	−0·592	−0·623	−0·664	−0·712	−0·771
25	−0·455	−0·552	−0·775	−0·825	−0·859	−0·922	−0·969
30	−0·435	−0·574	−0·981	−1·040	−1·077	−1·087	−1·044
40	−0·387	−0·648	−1·388	−1·362	1·287	−0·965	$2{\cdot}485^{-2}$
50	−0·381	−0·795	−2·410	2·906	1·580	1·257	1·128
60	−0·548	−1·011	2·070	1·851	1·667	1·492	1·372
70	−0·947	−1·281	1·820	1·697	1·526	1·365	1·216
80	−1·441	−1·706	1·710	1·586	1·451	1·284	1·07
90	−1·952	−2·300	1·626	1·440	1·291	1·160	1·03
100	−2·470	−2·894	1·552	1·318	1·126	0·985	0·85
110	−3·024	2·850	1·470	1·188	1·014	0·852	0·76
120	2·518	2·307	1·400	1·100	0·897	0·752	0·67
130	1·638	1·768	1·284	1·015	0·808	0·672	0·59
140	1·087	1·332	1·184	0·955	0·748	0·61	0·54
150	0·812	1·039	1·129	0·914	0·701	0·56	0·48
160	0·667	0·864	1·095	0·867	0·66	0·51	—
170	0·596	0·773	1·012	0·832	0·64	—	—

There are many calculations of λ and $|\chi|$ at 80 eV using several different methods (Madison and Calhoun 1978, Flannery and McCann 1975, Scott and McDowell 1975, Thomas *et al* 1974, Meneses *et al* 1978, Baluja and McDowell 1979). The distorted-wave calculations of Madison and Calhoun (1978), to which the data of Sutcliffe *et al* are normalised, give values of λ in good agreement with the data of Sutcliffe *et al* (1978); however they lie very much higher than the values obtained by Hollywood *et al* (1979). The many-body-theory calculations of Thomas *et al* (1974) and Meneses *et al* (1978) do not lie close to the measured values of λ and $|\chi|$. The most recent DW calculation of Baluja and McDowell (1979) does not agree with the experimental measurements of λ and $|\chi|$. The present R-matrix calculations of λ (also reported by our previous letter, Fon *et al* 1979b) are in agreement with the experimental data for small scattering angles. At larger angles they do not agree with the experiments of either Steph and Golden (1980) or Hollywood *et al* (1979); however they show quite clearly the minimum observed by Hollywood *et al* (1979) at 110°. The present R-matrix calculations of $|\chi|$ show remarkable agreement with the experimental data at small scattering angles. At larger scattering angles, the agreement between our calculation and experiment is not so good; however, our calculation appears to have the same shape as the experimental measurements of Steph and Golden (1980) and Hollywood *et al* (1979).

In figure 8, the present R-matrix calculations for λ and $|\chi|$ at 29·6 eV are compared with the experiments of McAdams *et al* (1979) and with the calculations of Scott (1976) and Thomas *et al* (1974). The two minima observed by Hollywood *et al* (1979) at 80 eV also show up at 29·6 eV for λ; while the first minimum becomes shallower at 50°, the second seems to be more pronounced and deeper than that shown at 80 eV. The sharp turning point for $|\chi|$ observed at 80 eV shifts to larger scattering angles at around 100°.

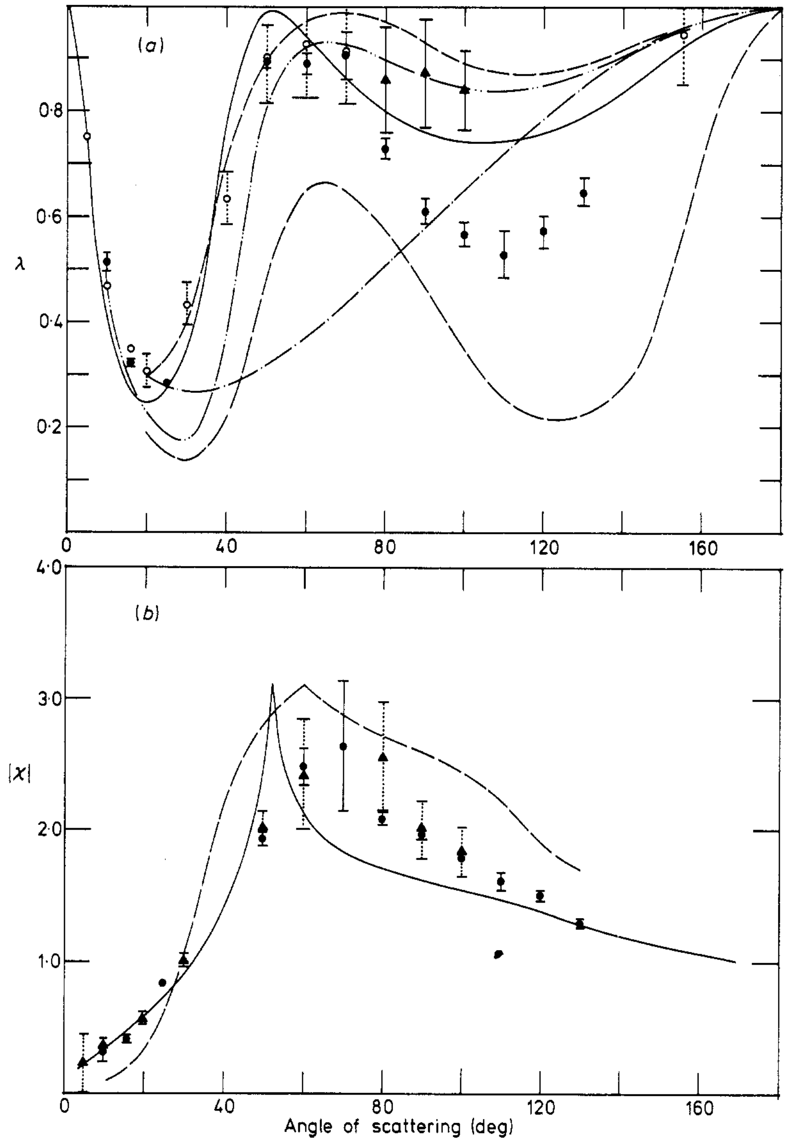

Figure 7. (λ, χ) parameters for 2^1P excitation at 81·63 eV, (*a*) λ, (*b*) $|\chi|$. Theory: ——, present R-matrix five-state calculation; – – –, Madison and Calhoun (1978); –·–·–, FBA; –··–, Meneses *et al* (1978); — —, Baluja and McDowell (1979). Experiment: ϕ, Sutcliffe *et al* (1978); ▲, Steph and Golden (1980); ●, Hollywood *et al* (1979).

The calculations of Thomas *et al* (1974) showing only one minimum do not reproduce the experimental shape of λ observed by McAdams *et al* (1979). The calculations of Scott (1976), though showing two minima, are again too small in comparison with the experiments. The present R-matrix calculations give λ values only slightly higher than that measured by McAdams *et al* (1979) and the position of minima and maximum are correctly predicted. The agreement between our calculated $|\chi|$ values and those measured by McAdams *et al* (1979) is good (see figure 8(*b*)).

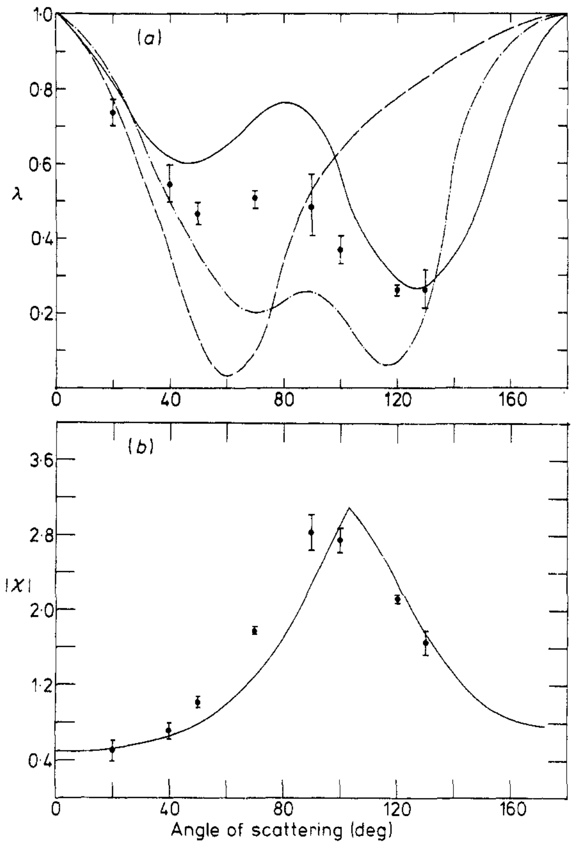

Figure 8. (λ, χ) parameters for 2^1P excitation at 29·6 eV (*a*) λ, (*b*) $|\chi|$. Theory: ——, present R-matrix five-state calculation; –·–·–, Scott (1976); — —, Thomas *et al* (1974). Experiment: ⧳, McAdams *et al* (1979).

The non-zero elements of alignment tensor A^{col} and orientation vector O^{col} given by (1), (2), (3) and (4) together with the θ_{min} defined by (6) are reported by our previous letter (Fon *et al* 1979b) at 80 eV. These same parameters at 29 eV are now shown and compared with the experimental data of McAdams *et al* (1979) in figure 9. We have also calculated the electron–photon correlation functions at 80 and 29·6 eV given by (5) and these are shown in figures 10 and 11. It is interesting to note that the calculated and measured electron–photon correlation functions are in better agreement than the values of λ and $|\chi|$ which are deduced from the observed electron–photon correlation functions.

4. Conclusions

The present R-matrix calculations are in very good qualitative agreement with the measured shapes of all the differential cross sections for all excitations of the $n = 2$ state of helium for all energies considered (see also Fon *et al* 1979a for the spin-forbidden excitations 2^3S and 2^3P). Quantitative agreement has also been achieved between our calculations and experiments for energies below 29·6 eV and above 100 eV. In

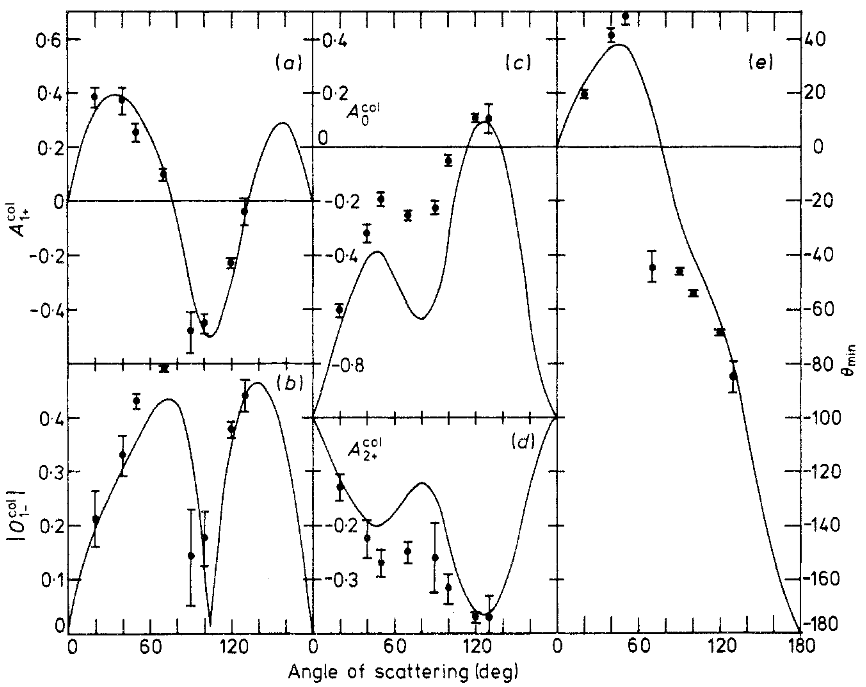

Figure 9. Electron excitation of 1^1S state of helium to 2^1P state at 29·6 eV. (*a*) A^{col}_{1+}; (*b*) $|O^{col}_{1-}|$; (*c*) A^{col}_{0}; (*d*) A^{col}_{2+} and (*e*) θ_{min} obtained from present *R*-matrix five-state calculations (——); and measurements of McAdams *et al* (1979): ⧳.

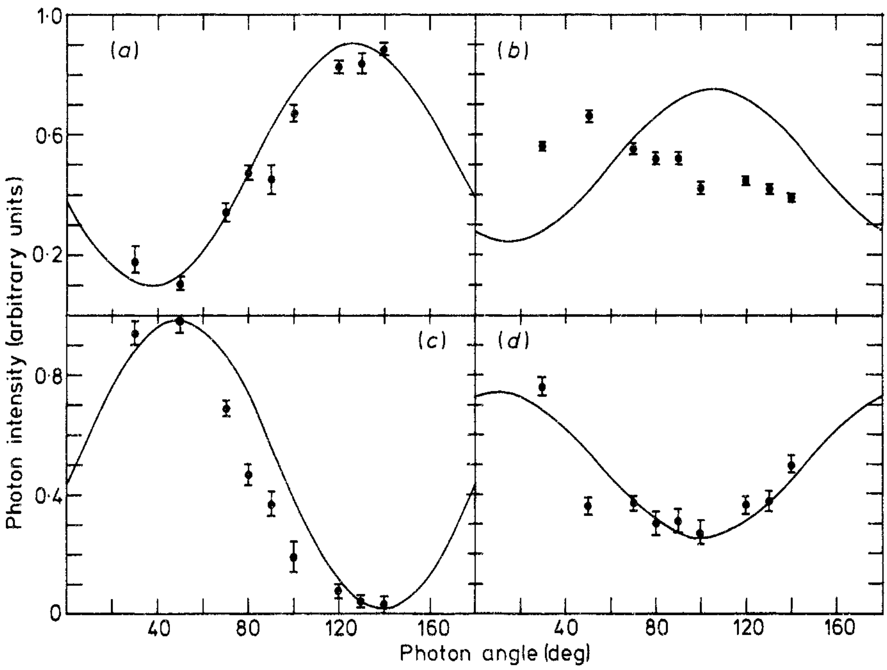

Figure 10. Electron–photon angular correlations for scattering angles (*a*) 40°; (*b*) 70°; (*c*) 100°; (*d*) 130° at 29·6 eV. The full curve is the present *R*-matrix calculations and the experimental points are the data obtained by McAdams *et al* (1979).

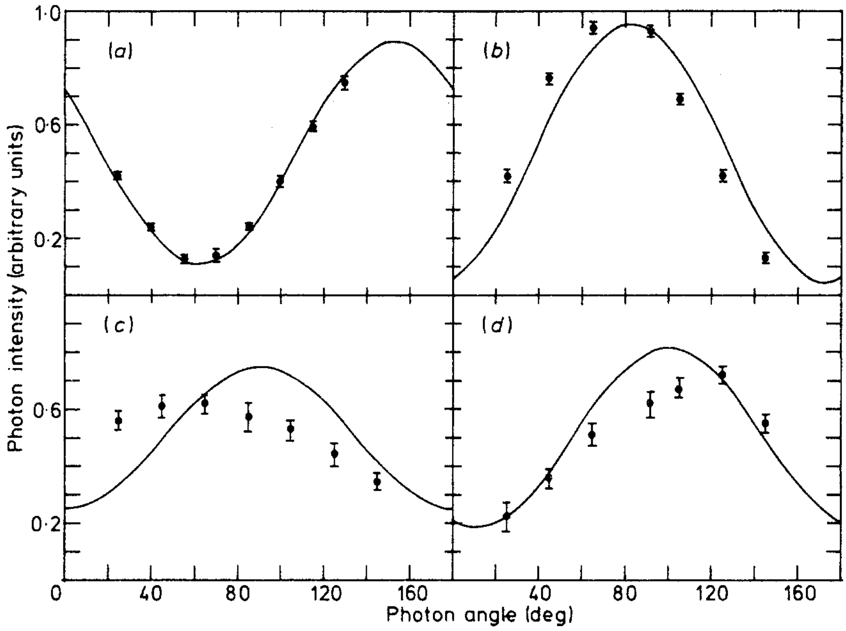

Figure 11. Electron–photon angular correlations for scattering angles (a) 25°; (b) 60°; (c) 100° (d) 130° at 81·6 eV. The full curve is the present R-matrix calculation and the experimental points are the data obtained by Hollywood *et al* (1979).

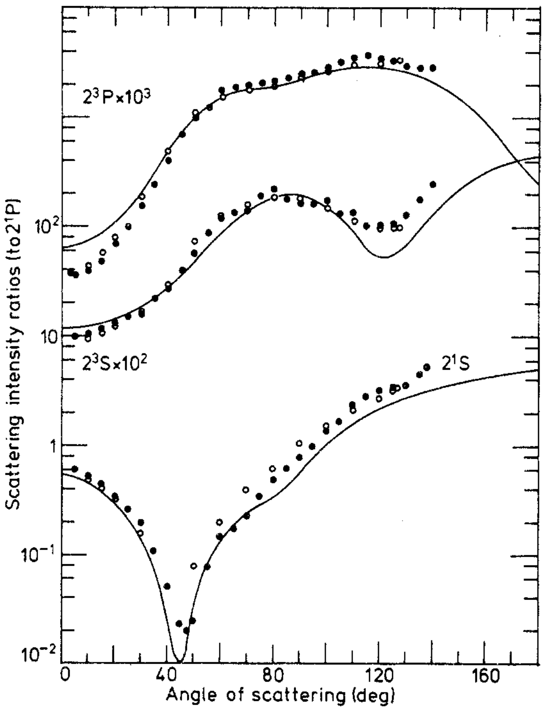

Figure 12. Scattering intensity ratios (to 2^1P) at 29·6 eV for 2^3P, 2^3S and 2^1S. Theory: ——, present R-matrix five-state calculation. Experiment: ○, Hall *et al* (1973); ●, Trajmar (1973).

addition the present calculations give all round satisfactory predictions for the λ and χ parameters observed in experiments (see also Fon *et al* 1979b).

It is interesting to note that in figure 5 our calculated differential cross section for $1^1S \rightarrow 2^1P$ at 29·6 eV are in remarkable agreement with the shape of the measured cross sections, but are approximately a factor of two higher. This is also true of our results for the excitation of ground state He to the 2^3S, 2^3P and 2^1S states. It would appear that our results would have been in excellent agreement with experiment if all the experiments were to be renormalised using the same normalising factor. In figure 12 the ratios of our calculated differential cross sections for $1^1S \rightarrow 2^3S$, $1^1S \rightarrow 2^1S$, $1^1S \rightarrow 2^3P$ transitions to that of the $1^1S \rightarrow 2^1P$ are compared with the ratios measured by Hall *et al* (1973) and Trajmar (1973) at 29·6 eV. There is remarkable agreement between our calculations and the experimental measurements. The difficulties of calibration in scattering experiments are well known (Moiseiwitsch and Smith 1968). However, one also notices that in atomic hydrogen, the 1s–2s and 1s–2p excitation cross sections are overestimated by a factor of two in 1s–2s–2p approximation in a similar energy range. Neglect of higher states not included in our expansion as indicated by the calculations of Bhadra *et al* (1979) might be the cause of the overestimation in our present calculation of the excitation cross sections.

Acknowledgments

We wish to thank Drs K H Winters and A Yagishita for sending us tabulated values of their cross sections and Drs A Crowe, M T Hollywood, J F Williams, R McAdams and N C Steph for sending us their experimental data in advance of publication. One of us (WCF) would like to acknowledge his gratitude of the Royal Society for an award of a Commonwealth Bursary and to the British Council (London) for a travel grant under the Commonwealth University interchange scheme. Most of the calculations were carried out using a link to the IBM 370/165 at the Daresbury Laboratory provided by a grant from the Science Research Council. We are particularly grateful to Professor P G Burke for his advice and encouragement throughout the course of this work.

References

Baluja K L and McDowell M R C 1979 *J. Phys. B: Atom. Molec. Phys.* **12** 835–46
Berrington K A, Burke P G and Sinfailam A L 1975 *J. Phys. B: Atom. Molec. Phys.* **8** 1459–73
Bhadra K, Callaway J and Henry R J W 1979 *Phys. Rev.* A **19** 1841–51
Bransden B H and McDowell M R C 1978 *Phys. Rep.* **46** 249–394
Bransden B H and Winters K H 1975 *J. Phys. B: Atom. Molec. Phys.* **8** 1236–44
Byron F W Jr and Joachain C J 1975 *J. Phys. B: Atom. Molec. Phys.* **8** L284–8
Chamberlain G E, Mielezarek S R and Kuyatt C E 1970 *Phys. Rev.* A **2** 1905–22
Chutjian A and Srivastava S K 1975 *J. Phys. B: Atom. Molec. Phys.* **8** 2360–8
Crooks G B 1972 *PhD Thesis* University of Nebraska
Dillon M A and Lassettre E N 1975 *J. Chem. Phys.* **62** 2373–90
Eminyan M, MacAdam K B, Slevin J and Kleinpoppen H 1974 *J. Phys. B: Atom. Molec. Phys.* **7** 1519–42
Fano U and Macek J H 1973 *Rev. Mod. Phys.* **45** 553–73
Flannery M R and McCann K J 1975 *J. Phys. B: Atom. Molec. Phys.* **8** 1716–33
Fon W C, Berrington K A, Burke P G and Kingston A E 1978 *J. Phys. B: Atom. Molec. Phys.* **11** 325–9
—— 1979a *J. Phys. B: Atom. Molec. Phys.* **12** 1861–72
Fon W C, Berrington K A and Kingston A E 1979b *J. Phys. B: Atom. Molec. Phys.* **12** L171–3

Gupta G P and Mathur K C 1979 *J. Phys. B: Atom. Molec. Phys.* **12** 1733–9

Hall R J, Joyez G, Mazeau J, Reinhardt J and Schermann C 1973 *J. Physique* **34** 827–43

de Heer F J and Jansen R J J 1977 *J. Phys. B: Atom. Molec. Phys.* **10** 3741–58

Hidalgo M B and Geltman S 1972 *J. Phys. B: Atom. Molec. Phys.* **5** 617–26

Hollywood M T, Crowe A and Williams J F 1979 *J. Phys. B: Atom. Molec. Phys.* **12** 819–34

Joachain C J and Winters K H 1977 *J. Phys. B: Atom. Molec. Phys.* **10** L727–30

McAdams R, Hollywood M T, Crowe A and Williams J F 1979 *Proc. 11th Int. Conf. on Physics of Electronic and Atomic Collisions* (Kyoto: Society for Atomic Collision Research) Abstracts p 168

Madison D H and Calhoun R V 1978 (results quoted by Sutcliffe *et al* 1978)

Madison D H and Shelton W H 1973 *Phys. Rev.* A **7** 499–513

Meneses G D, Padial N T and Csanak Gy 1978 *J. Phys. B: Atom. Molec. Phys.* **11** L237–42

Moiseiwitsch B L and Smith S J 1968 *Rev. Mod. Phys.* **40** 238–321

Opal C B and Beaty E C 1972 *J. Phys. B: Atom. Molec. Phys.* **5** 627–35

Pichou F, Huetz A, Joyez G, Landau M and Mazeau J 1976 *J. Phys. B: Atom. Molec. Phys.* **9** 933–44

Scott T 1976 *PhD Thesis* London University

Scott T and McDowell M R C 1975 *J. Phys. B: Atom. Molec. Phys.* **8** 1851–65

—— 1976 *J. Phys. B: Atom. Molec. Phys.* **9** 2235–54

Steph N C and Golden D E 1980 *Phys. Rev.* submitted

Sutcliffe V C, Haddad G N, Steph N C and Golden D E 1978 *Phys. Rev.* A **17** 100–7

Suzuki H and Takayangi T 1973 *Proc. 8th Int. Conf. on Physics of Electronic and Atomic Collisions* (Belgrade: Institute of Physics) Abstracts p 286

Tan K H, Fryar J, Farago P S and McConkey J W 1977 *J. Phys. B: Atom. Molec. Phys.* **10** 1073–82

Terebey J Z 1974 *J. Phys. B: Atom. Molec. Phys.* **7** 460–7

Thomas L D, Csanak Gy, Taylor H S and Yarlagadda B S 1974 *J. Phys. B: Atom. Molec. Phys.* **7** 1719–33

Trajmar S 1973 *Phys. Rev.* A 191–203

Truhlar D G, Trajmar S, Williams W, Ormond S and Torres B 1973 *Phys. Rev.* A **8** 2475–82

Ugbabe A, Teubner P J O, Weigold E and Arriola H 1977 *J. Phys. B: Atom. Molec. Phys.* **10** 71–9

Westerveld W B, Heideman H G M and Van Eck J 1979 *J. Phys. B: Atom. Molec. Phys.* **12** 115–35

Winters K H, Issa M R and Bransden B H 1977 *Proc. 10th Int. Conf. on Physics of Electronic and Atomic Collisions* (Paris: Commissariat à l'Energie Atomique) Abstracts p 424

Yates A C and Tenney A 1972 *Phys. Rev.* A **6** 1451–6